ISBN: 978-3-95450-227-1 ISSN: 2673-5490 doi:10.18429/JACoW-IPAC2022-TUPOPT039

CHARACTERIZATION OF DIAMOND WITH BURIED BORON-DOPED LAYER DEVELOPED FOR Q-SWITCHING AN X-RAY OPTICAL CAVITY*

R. A. Margraf† [1], J. Krzywinski, T. Sato, J. P. MacArthur, D. Zhu, M. L. Ng, A. Halavanau, R. Robles[1], A. Robert[2], Z. Huang[1], G. Marcus, SLAC, Menlo Park, USA
M. D. Ynsa, Center for Micro Analysis of Materials, Autónoma, Madrid, Spain
F. Ke, Stanford University, Stanford, USA
S.-K. Mo, Y. Zhong[1], Lawrence Berkeley National Laboratory, Berkeley, USA
P. Pradhan, Argonne National Laboratory, Lemont, USA
[1]also at Stanford University, Stanford, USA, [2]also at MAX IV, Lund, Sweden

Abstract

X-ray Free-Electron Laser Oscillators (XFELOs) and X-ray Regenerative Amplifier FELs (XRAFELs) are currently in development to improve longitudinal coherence and spectral brightness of XFELs [1]. These schemes lase an electron beam in an undulator within an optical cavity to produce X-rays. X-rays circulate in the cavity and interact with fresh electron bunches to seed the FEL process over multiple passes, producing progressively brighter and more spectrally pure X-rays. Typically, the optical cavities used are composed of Bragg-reflecting mirrors to provide high reflectivity and spectral filtering. This high reflectivity necessitates special techniques to out-couple X-rays from the cavity to deliver them to users. One method involves "Q-switching" the cavity by actively modifying the reflectivity of one Bragg-reflecting crystal. To control the crystal lattice constant and thus reflectivity, we use an infrared (IR) laser to heat a buried boron layer in a diamond crystal. Here, we build on earlier work [2] and present the current status of our Q-switching diamond, including implantation with 9 MeV boron ions, annealing and characterization.

INTRODUCTION

In Q-switching an optical cavity, as described in [2], an IR laser heats a region of a Bragg-reflecting mirror, actively modifying its reflectivity, and enabling out-coupling of X-rays. A crystal used for this purpose must have a uniform rocking curve (less than the rocking curve width of 8 µrad for 9.831 keV X-rays reflecting off diamond 400 planes) over a region the size of the X-ray beam ~40 µm. The crystal must also absorb IR light strongly. Diamond has thermal dissipation properties which make it ideal for use in in a cavity-based XFEL. A buried boron layer can be implanted to increase the IR absorption of diamond for Q-switching.

IMPLANTATION AND ANNEALING

A high-temperature-high pressure (HPHT) diamond, described in [2] was implanted as described in [3] with 9 MeV boron ions using the microbeam line at the Center for Micro Analysis of Materials (CMAM) at the Autonomous University of Madrid. 200 x 200 µm areas were implanted with fluences of 5×10^{15}, 1×10^{16},1.5×10^{16} 2×10^{16} and 2.5×10^{16} ions/cm^2 by scanning a focused beam of boron ions in a spiral rastering pattern.

Following implantation, five high-temperature in-vacuum annealings at 900, 950,1150, 1300, and 1450 °C were performed to heal implantation damage. 900 and 950 °C annealings were performed in a UHV chamber heated by a filament under 2.7×10^{-8} mbar or better vacuum. The filament was heated to the target temperature, then annealed for 1 hr. The 1150, 1300, and 1450 °C annealings were performed in a Red Devil G vacuum furnace manufactured by R. D. Webb Company Inc under 1×10^{-4} mbar or better vacuum, similar to [4]. The furnace was ramped up at 2 °C/min, annealed for 3 hr, then ramped down at 3 °C/min to 700 °C and cooled.

During this process, we did see some graphitization, as shown in Fig. 1, but not on our regions of interest.

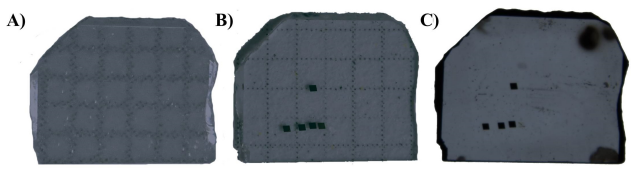

Figure 1: 1x images of HPHT diamond. A) Pre-implantation, B) Post-implantation, Post 1450 °C annealing.

CHARACTERIZATION

We performed several measurements to characterize healing in the boron-implanted regions.

IR Transmittance

To show implantation increases IR absorption, we measured IR transmittance. A Thorlabs CPS780S laser diode beam was expanded, collimated and transmitted through our sample. A Thorlabs FL780-10 780 nm filter selected the signal wavelength before a Mako G-319C POE camera.

The post 1450 °C annealing case is shown in Fig. 2. The IR transmittance of un-implanted diamond and the region of lowest doping is similar, 66 - 69 %, and the more highly doped regions transmit less IR light, 15 - 26 %. To account for variation in transmittance across the diamond, we also

* This work was supported by the Department of Energy, Laboratory Directed Research and Development program at SLAC National Accelerator Laboratory, under contract DE-AC02-76SF00515.
† rmargraf@stanford.edu

ISBN: 978-3-95450-227-1 ISSN: 2673-5490 doi:10.18429/JACoW-IPAC2022-TUPOPT039

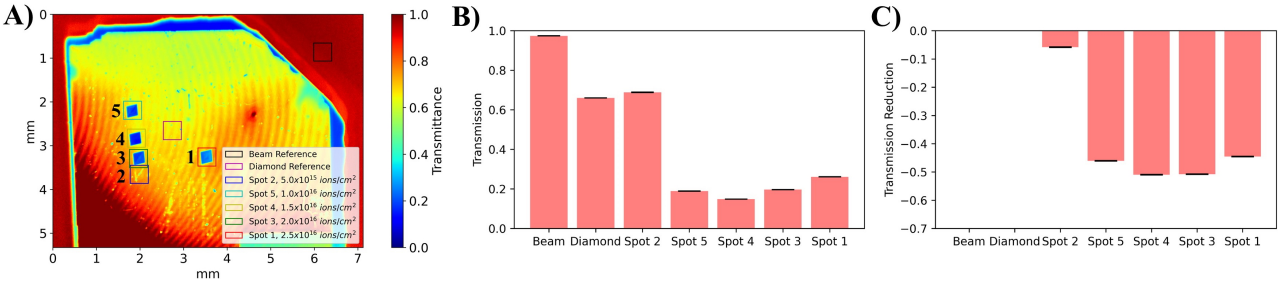

Figure 2: IR transmittance, post 1450 °C annealing. A) IR transmittance image. B) IR transmittance by region. C) Transmission of regions versus a region of un-doped diamond directly outside it. Error bars are standard error of the mean.

compared transmittance in each boron-implanted region to the un-implanted diamond directly surrounding it. We found the lowest doping reduced transmission of 6 %, versus 45 - 51 % for the highest doping. This suggests the least doped region absorbs only slightly more IR than pure diamond, while the highly doped regions absorb much more IR.

Micro-Raman Spectroscopy

To assess healing of boron-implanted regions, we performed micro-Raman spectroscopy. A Renishaw inVia Raman Microscope with a 514 nm laser and a Leica 20x/.40 N Plan Epi objective was used on a ~1 - 4 µm area spot.

Pure diamond has a sharp peak in the micro-Raman specta at 1332 cm^{-1}, as shown in Fig. 3. After implantation, the 1332 cm^{-1} peak decreased for all implanted regions. After 1450 °C annealing, the 1332 cm^{-1} peak for the lowest boron-doped region recovered to 83 % of the height of the diamond reference peak. However, the more highly boron-doped regions have a much smaller 1332 cm^{-1} peak, less than 3 % of the diamond reference peak. This suggests annealing at 1450 °C may somewhat heal the crystal lattice of a region doped with boron at a 5×10^{15} ions/cm^2 fluence, but higher fluences do not heal. Annealing also changes the micro-Raman background, consistent with earlier studies [5].

White-Light Topography

We performed a topography measurement on the implanted regions using a Zygo NewView, a 3d white light interferometer. For measuring the entire surface, stitching measurement was performed using a 2.75x objective.

As shown in Fig. 4, pre-annealing, the boron-implanted regions had a surface bulge of 50-160 nm. Post-annealing, the lowest boron-doped region decreased to a 10 nm bulge in some regions, while increasing to 100 nm on one edge. Additionally, annealing increased the surface bulge in the higher boron-doped regions. This suggests annealing promoted rearrangement of the diamond crystal lattice in the boron-implanted regions, and the diamond was not able to fully heal, especially in the highly doped regions.

Rocking Curve Imaging

To assess X-ray reflectivity in the Boron-doped regions, we performed RCI. The pre-annealing RCI was performed at the Advanced Photon Source at Argonne National Laboratory by reflecting 10 keV X-rays off diamond 400 lattice planes. The post 1450 °C annealing RCI was performed at beamline 10-2 of the Stanford Synchrotron Radiation Light Source at SLAC National Accelerator Laboratory by reflecting 9.831 keV X-rays off diamond 400 lattice planes [6]. Images were collected as the crystal was rotated, and a Gaussian fit was performed to find rocking curve center and FWHM.

In Fig. 5, annealing decreased overall deviation in the rocking curve center. It also decreased deviation of the rocking curve center in the implanted regions. However, even in the lowest boron-doped region there are still 10 µrad deviations in the rocking curve center, which are detrimental to Q-switching. We note that for pre-annealing dataset, the crystal was rocked left/right, versus up/down in the post 1450 °C dataset, explaining differences in RCI structure.

CONCLUSION

Characterization of the boron-implanted and 1450 °C annealed diamond showed moderate healing of the 5×10^{15} ions/cm^2 fluence region, and little healing at higher fluencies. While the increase in IR transmittance, recovery of the 1332 cm^{-1} micro-Raman peak, and reduction in surface bulge in white-light topography are all signs of healing in the lowest doped region, the 10 µrad deviations in RCI still make the diamond challenging for Q-switching use.

In future work, we must increase uniformity of the RCI within the boron-doped regions while keeping IR absorption high. The structure in the RCI within the boron-doped regions is likely due to implanting ions in a rastering pattern. For a more uniform RCI, future studies should use a large ion beam with a mask, rather than rastering. To avoid reduction in IR absorption with annealing, one might forgo annealing and reflect off the opposite surface of the crystal. The back is less damaged by the boron implantation, as boron ions passed through the front as they were implanted in the crystal. One could machine a diamond drumhead from the back surface of the crystal such that the boron-implanted regions are 5 µm below the reflecting surface.

Future diamond boron-implantions should produce a uniform RCI, enabling Q-switching of a cavity-based XFEL.

ISBN: 978-3-95450-227-1 ISSN: 2673-5490 doi:10.18429/JACoW-IPAC2022-TUPOPT039

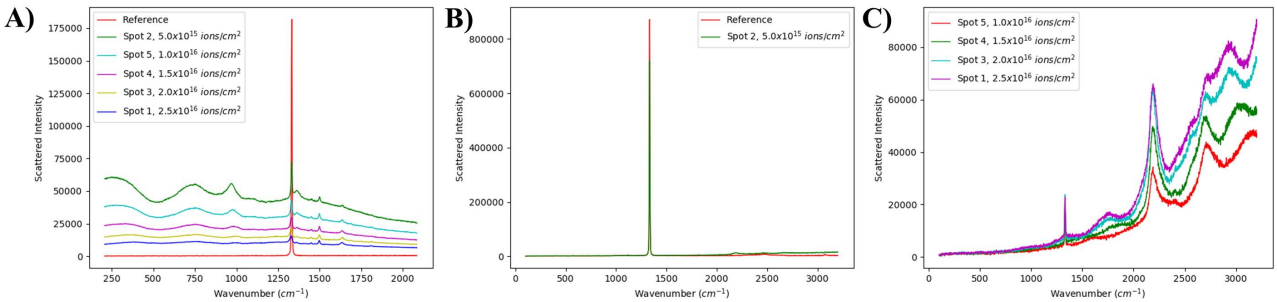

Figure 3: Micro-Raman Spectroscopy. A) Pre-annealing, B-C) post 1450 °C annealing.

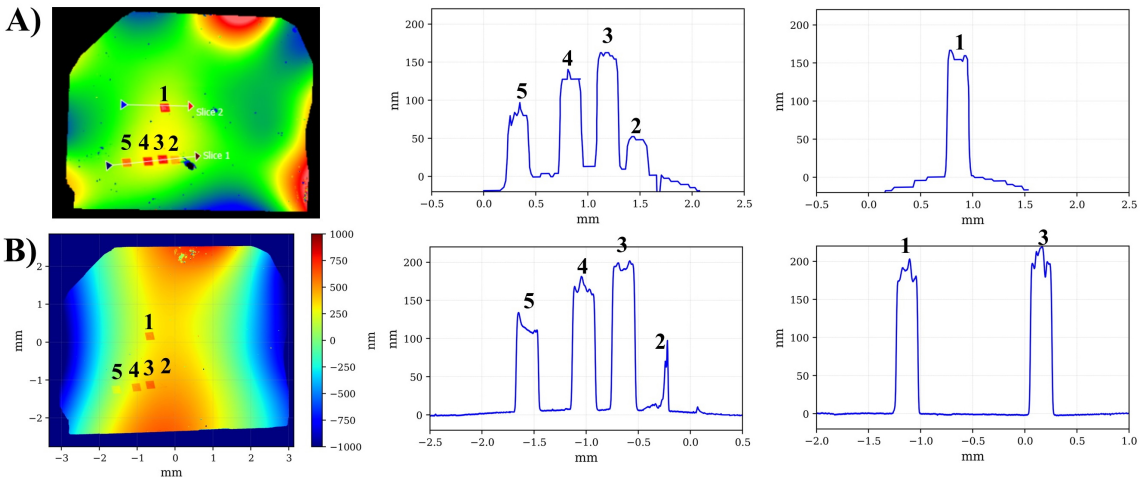

Figure 4: White light topography. Left plots show surface height across full area of crystal, center and right plots show line scans where a quartic background term has been removed. A) Pre-annealing, B) post 1450 °C annealing.

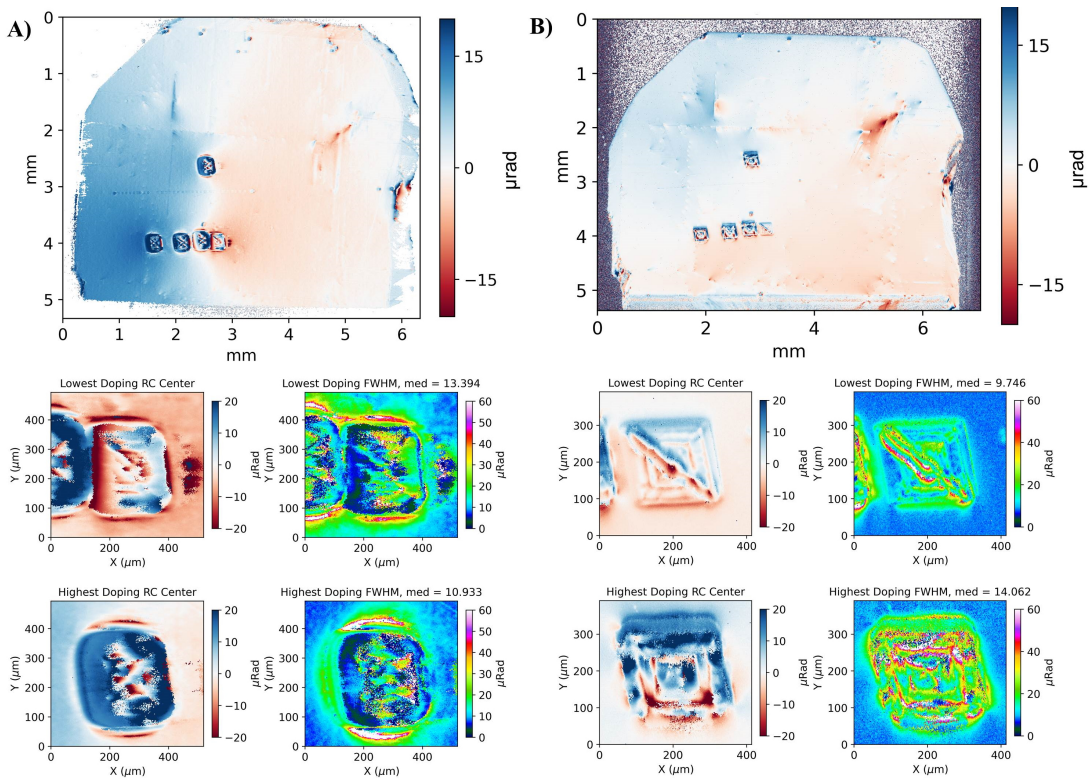

Figure 5: RCI Imaging, including RCI center and FWHM for spots 2 and 1. A) Pre-annealing, B) post 1450 °C annealing.

ISBN: 978-3-95450-227-1 ISSN: 2673-5490 doi:10.18429/JACoW-IPAC2022-TUPOPT039

REFERENCES

[1] Gabriel Marcus *et al.*, "CBXFEL Physics Requirements Document for the Optical cavity Based X-Ray Free Electron Lasers Research and Development Project." SLAC, CA, USA, SLAC-I-120-103-121-00, Apr. 2020.

[2] J. Krzywi *et al.*, "Q-Switching of X-Ray Optical Cavities by Using Boron Doped Buried Layer Under a Surface of a Diamond Crystal", in *Proc. FEL'19*, Hamburg, Germany, Aug. 2019, pp. 122–125. doi:10.18429/JACoW-FEL2019-TUP033

[3] M.D. Ynsa, M.A. Ramos, N. Skukan, V. Torres-Costa, and M. Jakšić, "Highly-focused boron implantation in diamond and imaging using the nuclear reaction ^{11}B(p, α)^{8}Be," *Nucl. Instrum. Methods Phys. Res., Sect. B*, vol. 348, pp. 174–177, Apr. 2015. doi:10.1016/j.nimb.2014.11.036

[4] P. Pradhan *et al.*, "Small Bragg-plane slope errors revealed in synthetic diamond crystals," *J. Synchrotron Rad.*, vol. 27, no. 6, pp. 1553–1563, Nov. 2020. doi:10.1107/S1600577520012746

[5] M. D. Ynsa, F. Agulló-Rueda, N. Gordillo, A. Maira, D. Moreno-Cerrada, and M. A. Ramos, "Study of the effects of focused high-energy boron ion implantation in diamond," *Nucl. Instrum. Methods Phys. Res., Sect. B*, vol. 404, pp. 207–210, Aug. 2017. doi:10.1016/j.nimb.2017.01.052

[6] A. Halavanau *et al.*, "Rocking Curve Imaging Experiment at SSRL 10-2 Beamline", in *Proc. IPAC'21*, Campinas, Brazil, May 2021, pp. 357–360. doi:10.18429/JACoW-IPAC2021-MOPAB096